International Journal of Chemical and Biochemical Sciences
(ISSN 2226-9614)

Journal Home page: www.iscientific.org/Journal.html

Microstructural Insights and Composition Analysis of a Fractured Brass Alloy of Unknown Composition Using Advanced Characterization Techniques

Saira Bano[1], Muhammad Arshad[2], Naseer Ahmed Khan[3], Naveed ul Hasan Syed[4], Samiul Haq[5]*

[1-5]*Department of Chemical Engineering, University of Engineering and Technology (UET) Peshawar, Khyber Pakhtunkhwa (KPK) 25120, Pakistan*

Abstract

This study aims to investigate the microstructural and compositional characteristics of a fractured brass alloy using energy-dispersive X-ray spectroscopy (EDS), scanning electron microscopy (SEM), and X-ray diffraction (XRD). The brass alloy, initially of unknown composition, was determined to consist of 63.65 at% Cu, and 36.35 at% Zn through EDS analysis. Microstructural analysis via SEM revealed a typical ductile fracture pattern with necking and dimple formation, indicative of significant plastic deformation prior to failure. The alloy exhibited a grain size ranging from 10 µm to 80 µm and displayed both α-phase (FCC structure) and possible traces of β-phase, though XRD detected only the α-phase due to the low concentration of β-phase (<5%). A comparison between EDS and XRD results for analyzing chemical composition showed that good assumptions could be made from the lattice parameters of the binary alloy following Nelson-Relay function to predict an approximate composition in binary alloy systems, which was found to be 34 at% Zn in our analysis. Furthermore, the sample's crystal structure was confirmed as FCC, which supported its observed ductility and plastic deformation prior to fracture. The SEM analysis also confirmed that the material went through an annealing process. The fracture morphology further showed that the FCC structure and the annealing process both contributed to the material's increased ductility. The analysis further confirms that EDS is more reliable for chemical composition determination in an alloy system. Evidence of annealing twinning in the SEM images suggests the sample underwent an annealing process, contributing to its enhanced ductility.

Keywords: Alloys, Chemical Composition, Failure Analysis, Materials, Microanalysis.

Full length article *Corresponding Author, e-mail: syednaveed@uetpeshawar.edu.pk Doi # https://doi.org/10.62877/16-IJCBS-24-26-20-16

1. Introduction

The significance of characterizing unknown materials extends far beyond academic curiosity. For instance, accurate identification and characterization of materials can be the basis for solving a complex case that spans from tracing the origins of a specific metal fragment to detecting contaminants in substances [1]. Similarly in industries, quality control is the most critical function to ensure that the product is consistent, safe, and reliable. Failure to characterize a material can led to reproduction of the products, financial losses, and sometimes even user safety hazards [2]. More important, in today's age, moving into the future with custom-designed materials for specific applications, the need for widespread characterization and understanding of new and novel materials is necessary [3]. Results can be unexpected if parts fail unexpectedly during industrial processes. It is no longer necessarily, just an issue of understanding failure but also looking at ways that could be used to prevent such failures in future, as well as understanding broader implications of such failures within similar environments or applications [4]. Tensile testing and other mechanical tests give information on behavior of a material concerning strength, ductility, and other mechanical characteristics. However, these tests often provide a macroscopic view and deal with bulk material properties.

Material characterization will be inevitable in understanding the objective complexity concerning material behavior, specifically at the micro-nano scale. Mechanical tests can have their information complemented by SEM, EDX, and XRD, among other techniques, which give detailed insight into the microstructure, chemical composition, and crystalline arrangement of the material [6]. Materials

characterization shows intricate details of the material's microstructure and gives an understanding of detailed reasons for its performance and behaviors. After investigating the microstructural arrangements, researchers with these materials may identify areas of stress concentration, dislocation movements, grain boundary interaction that might have contributed to the observed deformations during failure [5]. Such detailed insights of the materials are just beyond the superficial examination as it provides a lens into its entire lifecycle. Understanding a material involves much more than the knowledge of its current state or the consequence of a failure incident. It is also defined by the material's history and the processes it has gone through, as well as the effects of those processes. For instance, material processing with heat makes an annealing process that leads to recrystallization, grain growth, or relief of internal stresses.

It then plays a major part in determination of final microstructure of a material [7]. Generally, those changes show up by specific microstructural features. One of these is twinning, a crystal defect where two parts of a crystal lattice are mirror images. Existence of twins will give practitioner an indication of plastic deformation and point out possible specific annealing conditions, thus becoming a crucial clue of material's processing history [8]. Due to its versatility, brass is enormously indebted to a lot of its uniqueness, which is driven by its varied compositions. Microstructural complexity of brass generally indicates internal arrangements of its composition in main influenced areas, heavily influenced by its zinc (Zn) content. For instance, brass alloys up to a composition of 34.36 at% Zn predominantly exhibit one phase, called single α-phase. This α-phase possesses properties of a face-centered cubic (FCC) structure and is ductile and malleable, thus fit for shaping processes [9]. A slightly higher Zn content of up to 36.35 at% can be found in α-phase brass with careful processing techniques such as controlled annealing and cooling rates. At relatively high Zn contents, especially within composition range of 31.39 – 38.35 at. %, microstructure turns out to be more complex, showing both α and β-phases simultaneously [10].

The occurrence of the β-phase in the BCC structure shifts the mechanical properties at room temperatures. With a correspondingly high level of the β-phase, especially at brass compositions higher than 38.35 at% Zn, hardness becomes significantly high. This hardness is suitable for wear resistance and specific other applications, but it takes alloy's ductility away. In such a way, the alloy demonstrates superior strength properties; therefore, it is right here to be used in cases where strength is more critical than formability [11]. This research paper aims to characterize and analyzed a fractured brass alloy sample of unknown composition. Advanced materials characterization tools such as EDX chemical analysis, SEM imaging, and XRD structural analysis have been used to find fracture mechanism behind the specimen failure. Fracture behavior is inextricably associated with microstructural details of materials. Thus, brass sample is investigated to understand intricate interplay between microstructure, composition, and fracture behavior. These insights, facilitated by analysis of surface morphology, compositional mapping, and structural determinations, give an overall view of material properties. This comprehensive approach will not only enhance understanding of this specific alloy but also provide a blueprint for similar further investigations.

2. Methodology

A total of two alloy samples were prepared for SEM analysis. The as received alloy specimen was sectioned. The sample with the fractured surface was used to investigate failure analysis, whereas the polished sample was used to assess the bulk alloy microstructure and its processing history. The surface of the cut sample was prepared using fine grinding and then polishing with Alumina suspension (particle size 300 nm) and colloidal silica (particle size 50 nm) as per standard metallographic technique and using a Buehler AutoMet-300 (Lake Bluff, USA). Microstructural analysis of the samples was done using an FEI XL.30 scanning electron microscope (SEM) having a Tungsten filament electron source and equipped with an EDX detector. The high-resolution imaging capabilities of the SEM are instrumental in revealing fractured topographical surface features of the fractured sample surface. SEM images of both surfaces, bulk alloy surface and fractured surface, of the samples were obtained to investigate fracture type and fracture mechanism. Both secondary electron (SE) imaging and backscattered electron (BSE) imaging were conducted on both polished and fractured surfaces. These images revealed valuable insights into the intricate details of microstructure and surface morphology. BSE images of fractured surface exhibit important information about type of fracture, fracture mechanism, and force type that led to cause fracture.

These images helped in understanding the physical changes the alloy specimen experienced during the fracture process. EDX with accompanying software INCA micro-analysis system was used for chemical analysis of unknown alloy sample. Chemical quantification of the provided sample was done using pure Cu and Zn to act as a benchmark for the brass alloy sample. EDX scans were done with an accelerating voltage of 20kV to determine the elemental composition of the material. EDX mapping was done to determine the distribution of elements across the sample's surface and to identify any chemical in homogeneities that may exist. Additionally, line scan was employed to take a more detailed image of the elemental distribution along the path on the sample surface. X-ray Diffractometer (Bruker Advance) with CuKα radiation was used for phase composition and structural analysis of the sample. The sample was loaded into the sample holder and exposed to x-rays radiation. The resulting XRD scan from the sample was obtained in 2θ range of 40° to 140° at a scan rate of 0.4 sec/step with an increment of 0.01°. The acquired diffractogram was analyzed for crystal structure, and as well as for the chemical composition of this binary solid solution.

3. Results and discussion

3.1. Microstructure Analysis

Figure 1(a) illustrates a Secondary Electron (SE) image of a polished brass sample that has revealed certain significant features like the size of grains, orientation, shapes, types, and grains. The equiaxed structure of the grain in the sample shows uniform solidification of the alloy during processing, with the varied grain sizes in a range of 10 to 80 μm in diameter. In the figure, a large grain size is denoted by the fact that re-growth occurred in some of the crystals, and this increased with an increase in the annealing time. The increase in ductility in this case is also due to the annealing treatment. Figure 1(b) is a BSE compositional contrast with the mapping of a solid-solid solution specimen; bright areas

are the region containing copper (Z = 29), in contrast to the zinc (Z = 30) because of its high atomic number. That increases the atomic number by one from the zinc to the copper and gives the notable difference in image contrast. This is because copper produces a greater intensity of backscattered electrons than zinc; therefore, it enables the differentiation between the presences of the two elements in compositional contrast mapping.

Clear geometrical grains structures and their location indicate the likely occurrence of single α-phase brass. As of the grain orientation shown in the image, its random location shows an isotropic property of this solid-solid solution. The randomly formed darker spots could behave as a nucleation site for the initial formation of the β-phase or impurities. Straight-sided bands running across grains in **Error! Reference source not found.**(a) shows a nnealing twinning. The reason for twinning can be attributed to the fact that the brass alloy sample underwent some annealing work as suggested by [2] and giving idea about material processing history. During annealing, the atoms in the metal rearrange themselves into a more stable and organized structure, which can lead to the formation of twinned crystal structures in some materials for instance materials of high stacking fault energy. Twinning is basically the different orientation of the crystal structures of same atomic arrangement within the same grain. Twinning can be desirable and predictable, and it can affect mechanical properties in some cases it can be a problem, as it can lead to cracking and other forms of failure in metals [1].

3.1. Failure Analysis

For fractography analysis, the fractured sample's images by Secondary Electron (SE) is presented in Figure 2. The fractographs in Figure 2(a-b) are taken on the plane perpendicular to the applied load/stress. It is essential to mention that the sample is tilted about 30° to the vertical axis of the page. Tilting specimen is done because fractures often occur at an angle to the surface which make it difficult to get a clear view of the fractured surface topography and morphology [2]. In **Error! Reference source not found.**(a) a t 500 µm scale the specimen is tilted and it shows graphical illustration of fractured surface. In this image at lower magnification the edges are curved towards the center of the specimen which shows necking during fracture process. In the middle of the specimen at higher magnification in **Error! R eference source not found.**(b) shows many spherical dimples of different sizes which shows that the material underwent ductile fracture, indicating that it deformed plastically before failing. The presence of different sized dimples suggests that there were variations in the local stress and strain conditions during the deformation process. Steps involved in the fracture process is explained later and graphically illustrated in **Error! Reference source not f ound.**.

Fracture process is a sequence of events that occurs in material when it underwent failure due to an external load or stress. **Error! Reference source not found.** shows the c omplete fracture process under the influence of an applied tensile load. It shows that necking is the first step starts under the applied stress and is followed by small cavities and micro-voids in the interior. When a material undergoes tensile deformation, the atomic bonds between neighboring atoms are stretched, causing localized areas of strain. As the strain in these regions reaches a critical level, micro-voids start to form, resulting in small areas of localized deformation within the material. These micro-voids then grow and coalesce to form larger voids, as observed in Figure 3 (void growth and linkage) as elliptical crack is formed that is perpendicular to the applied stress. Cracks propagation propels due to further merging of cavities and micro-voids. Finally, the rapid propagation of cracks around the outer surface completes the fracture process[3]. The inset in the **Error! Reference source n ot found.** bottom left shows the magnified image of the cracked surface revealing the topographical features at micro-level gives details about the type of fracture.

Image in **Error! Reference source not found.** at r ight bottom shows that necking of the specimen occurred before fracture which is sign of the ductile fracture in ductile materials. Furthermore, ductile fracture is a typical surface contour of the obtained sample. It is called a cup-and-cone fracture because one of the connecting surfaces is cup shaped and the other is a cone shape [3]. At high enlargement, it can be seen that there are many dimples on surface, which are characteristics failure features due to uniaxial tensile failure [3]. The resulting dimples on the fracture surface are the direct result of the micro-voids that form during this process. Each dimple corresponds to half of void created in the fracture process. The presence of these dimples is a clear indication that the material underwent significant plastic deformation prior to fracture, and therefore it can be identified as a ductile fracture. This type of fracture is often seen in materials that can undergo significant deformation before failure, such as metals and certain polymers.

3.2. Chemical Analysis

Energy-dispersive X-ray spectroscopy (EDS) is a powerful analytical technique and was utilized to determine the relative amounts of elements present in our alloy sample. When using EDS, it is often more accurate to measure the counts of the pure elements in addition to the counts from the alloy [4]. **Error! Reference source not found.** demonstrates t he EDS spectrum attained from the sample of the alloy that shows the intensity/counts of the characteristic X-rays of the alloying elements which are zinc and copper. To measure sample chemical composition; characteristic X-rays produced from the alloy compared to the counts produced from the pure elements making up the alloy. X-ray net totals were acquired for pure copper, pure zinc as well as for the specimen in 50 seconds. Reading for each candidate was taken four times in the experiment and determine the mean count values. The relative amounts of the alloying elements were found by using determined mean specimen counts (N_{spec}) and standard counts (N_{std}) in the following Equation (1).

$$\text{Cspec} = \frac{\text{Nspec}}{\text{Nstd}} * (100) \qquad \textit{Equation (1)}$$

Error! Reference source not found. illustrates the q uantitative analysis and chemical composition of the unknown brass alloy sample. Based on the above Equation (1) concentration of Cu and Zn (C_{Zn} and C_{Cu}) in the sample was calculated as shown in the **Error! Reference source not f ound.**. Initial values obtained for Cu and Zn were 61.69 wt% and 36.42 wt%, respectively. These correspond to atomic

percentages of 63.55 at% for Cu and 36.45 at% for Zn. After normalisation, the values were found to be 62.88 wt% for Cu and 37.12 wt% for Zn, corresponding to atomic percentages of 63.56 at% for Cu and 36.44 at% for Zn. The certified nominal composition of the sample was 63 wt% Cu and 37 wt% Zn, or 63.65 at% Cu and 36.35 at% Zn.

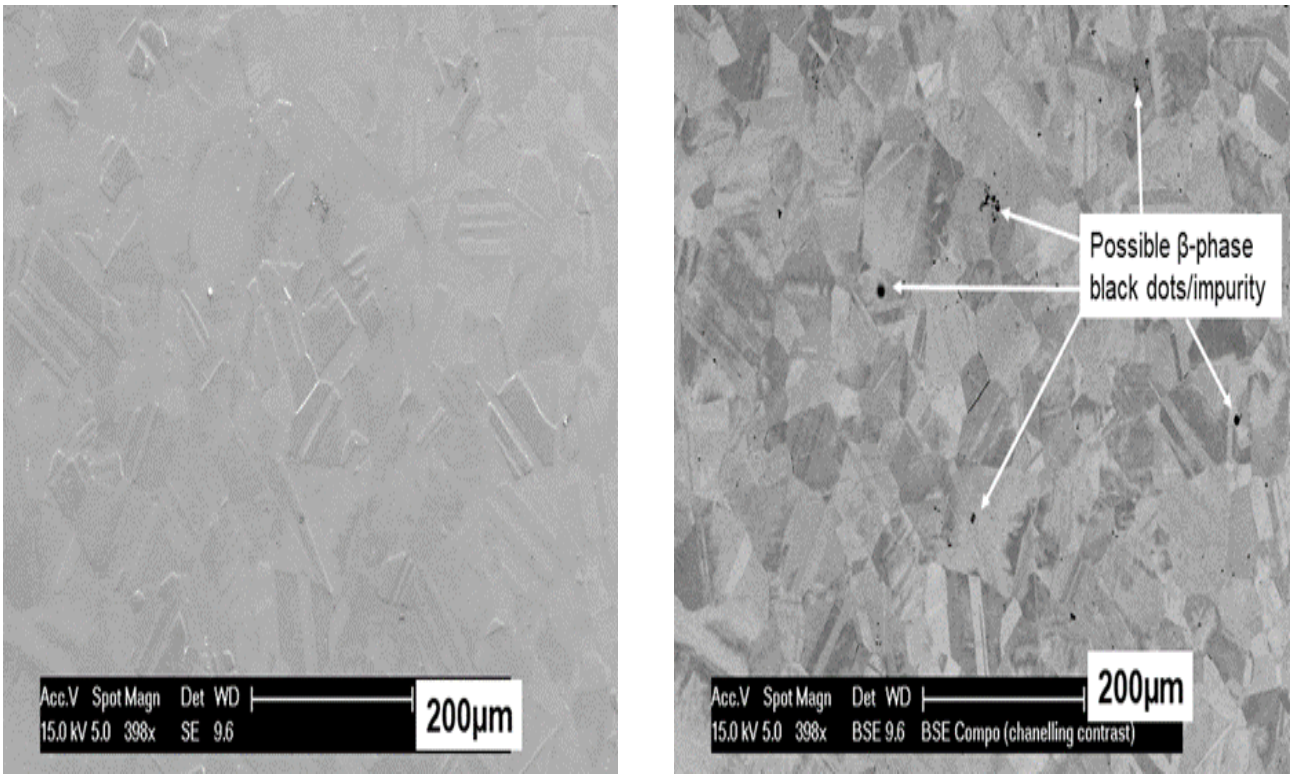

Figure 3.1. (a) Secondary Electron image of polished brass sample, (b) Backscattered Electron (BSE) image of polished specimen.

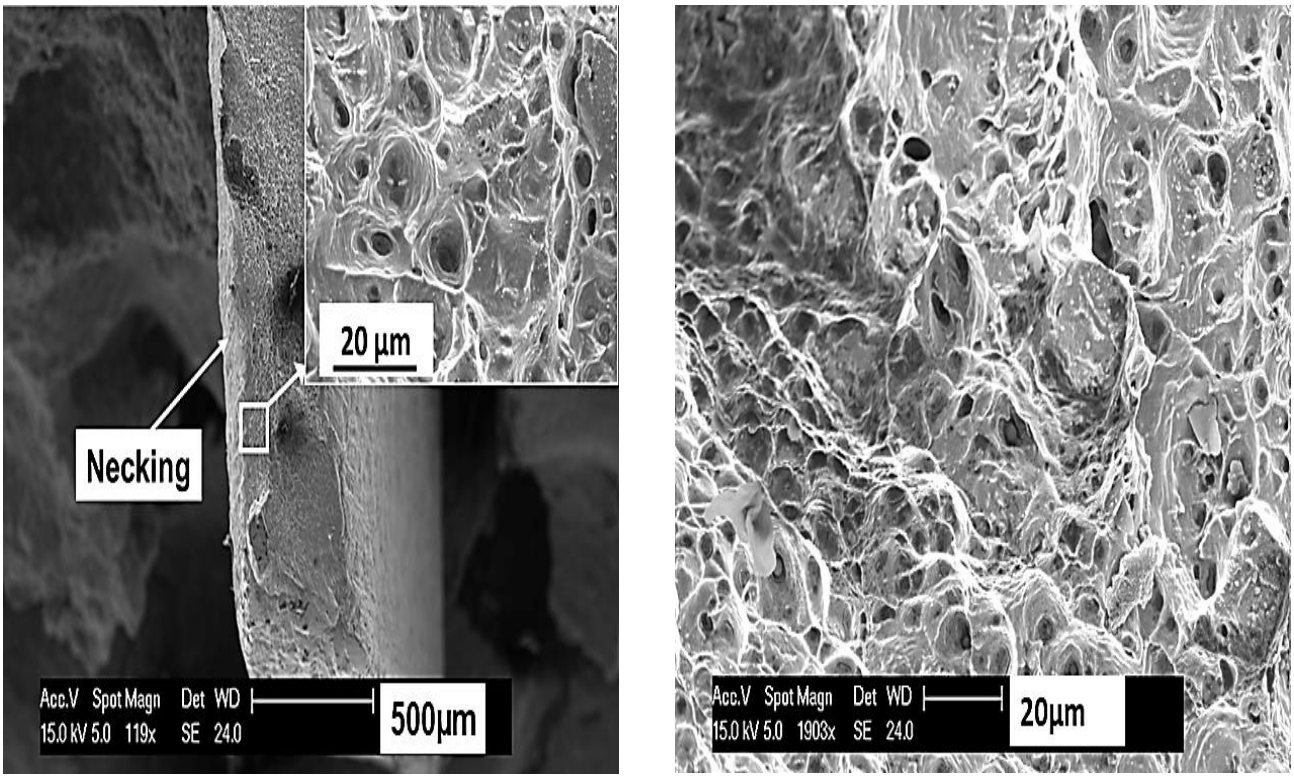

Figure 3.2. (a) SE SEM image of fractured specimen with magnified inset view, (b) SE SEM image of fractured brass sample

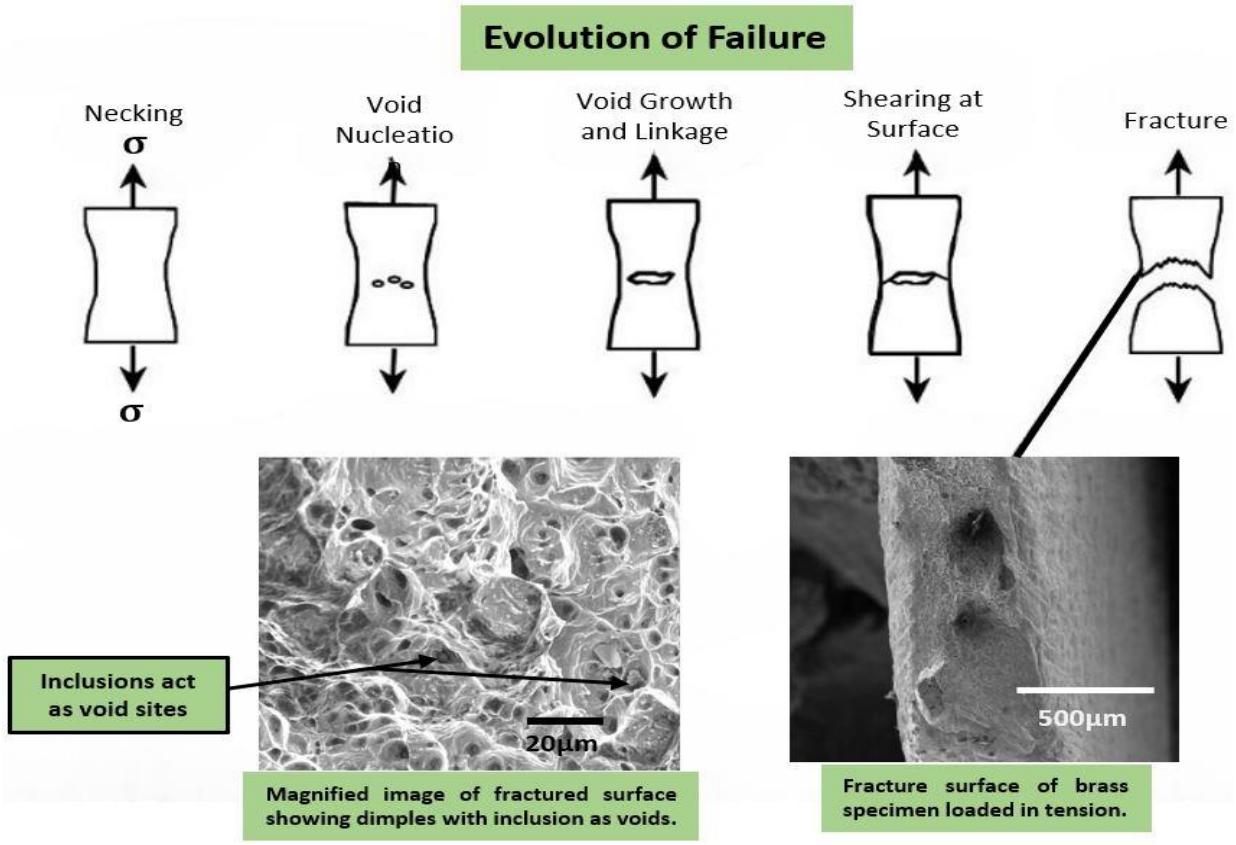

Figure 3.3. Crack propagation mechanism started from cracking following a series of steps before ending on fracture/failure.

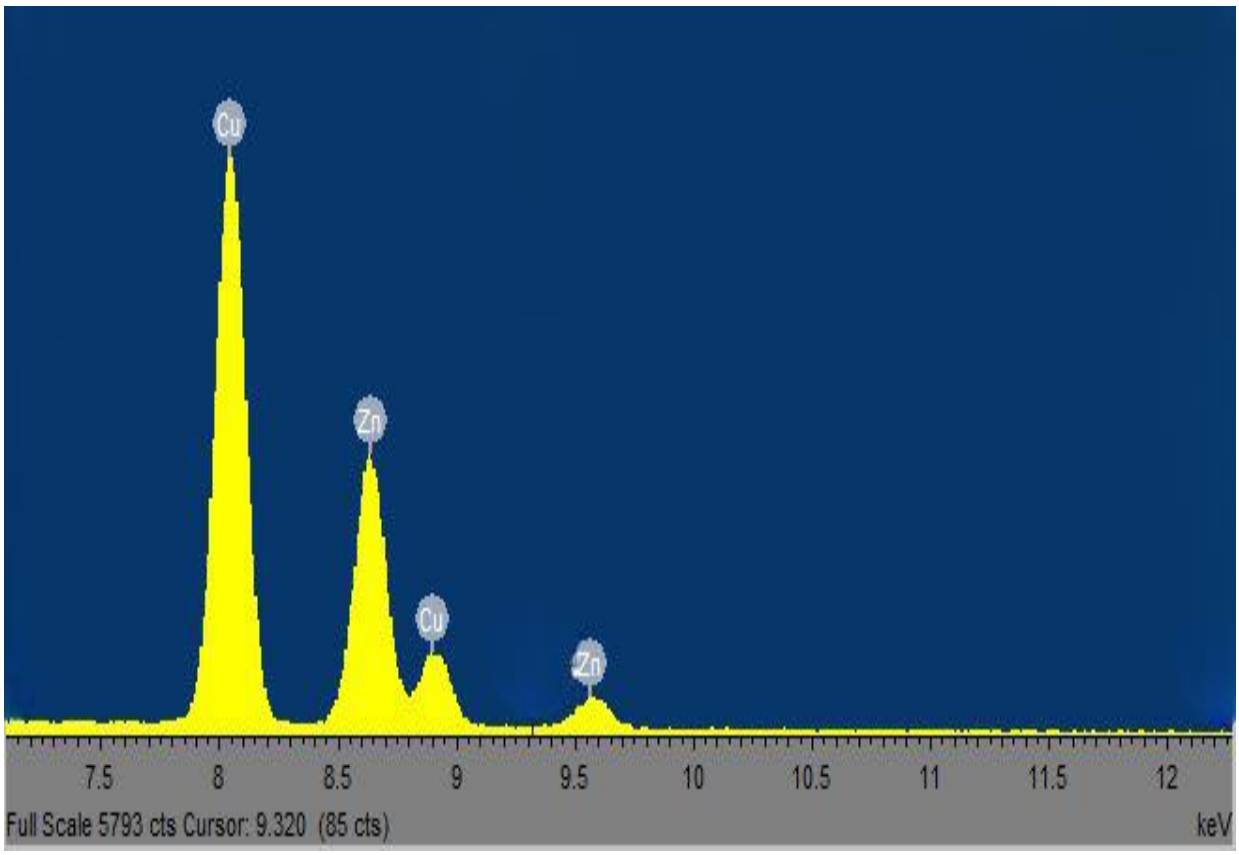

Figure 3.4. Shows EDS spectrum of point analysis from brass sample.

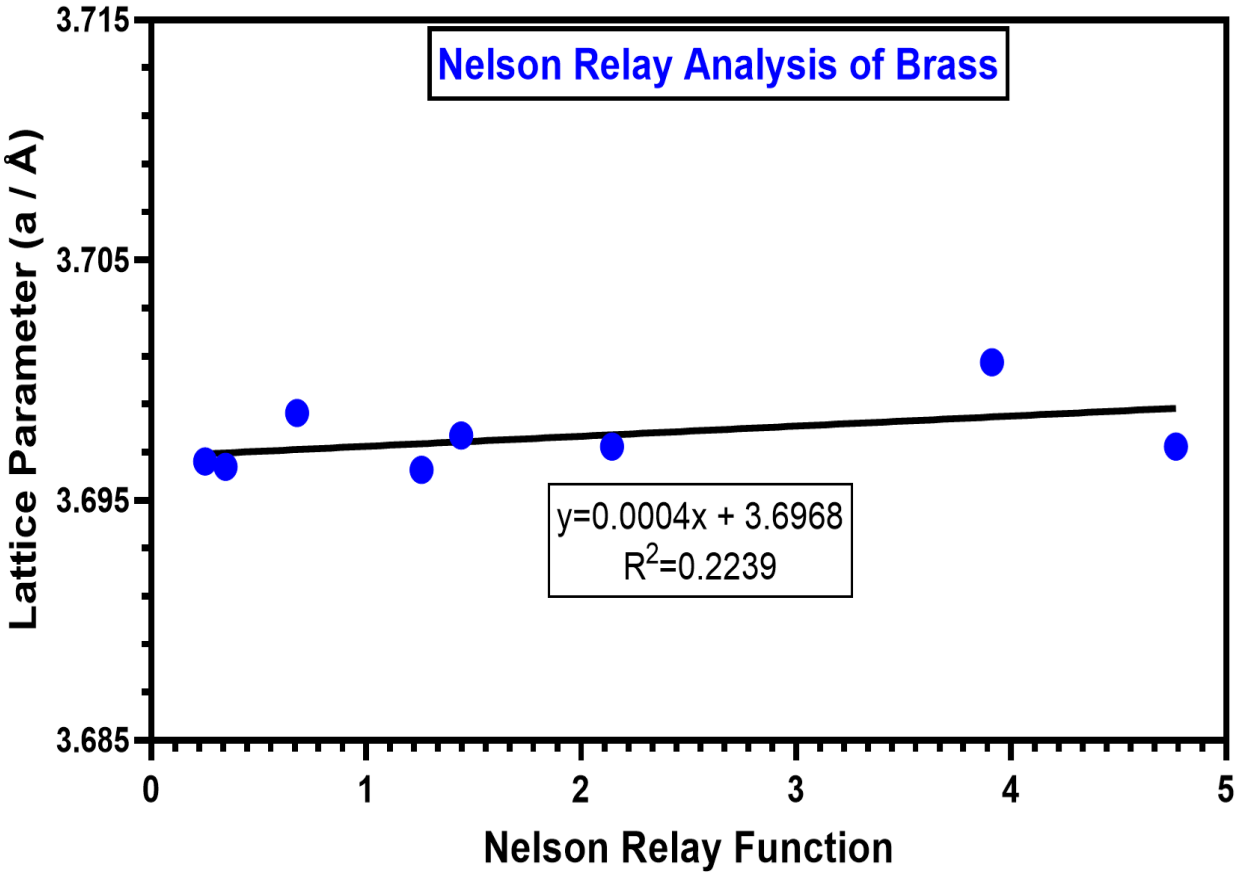

Figure 3.5. Determination of the lattice parameter by reduction against the Nelson-Riley function.

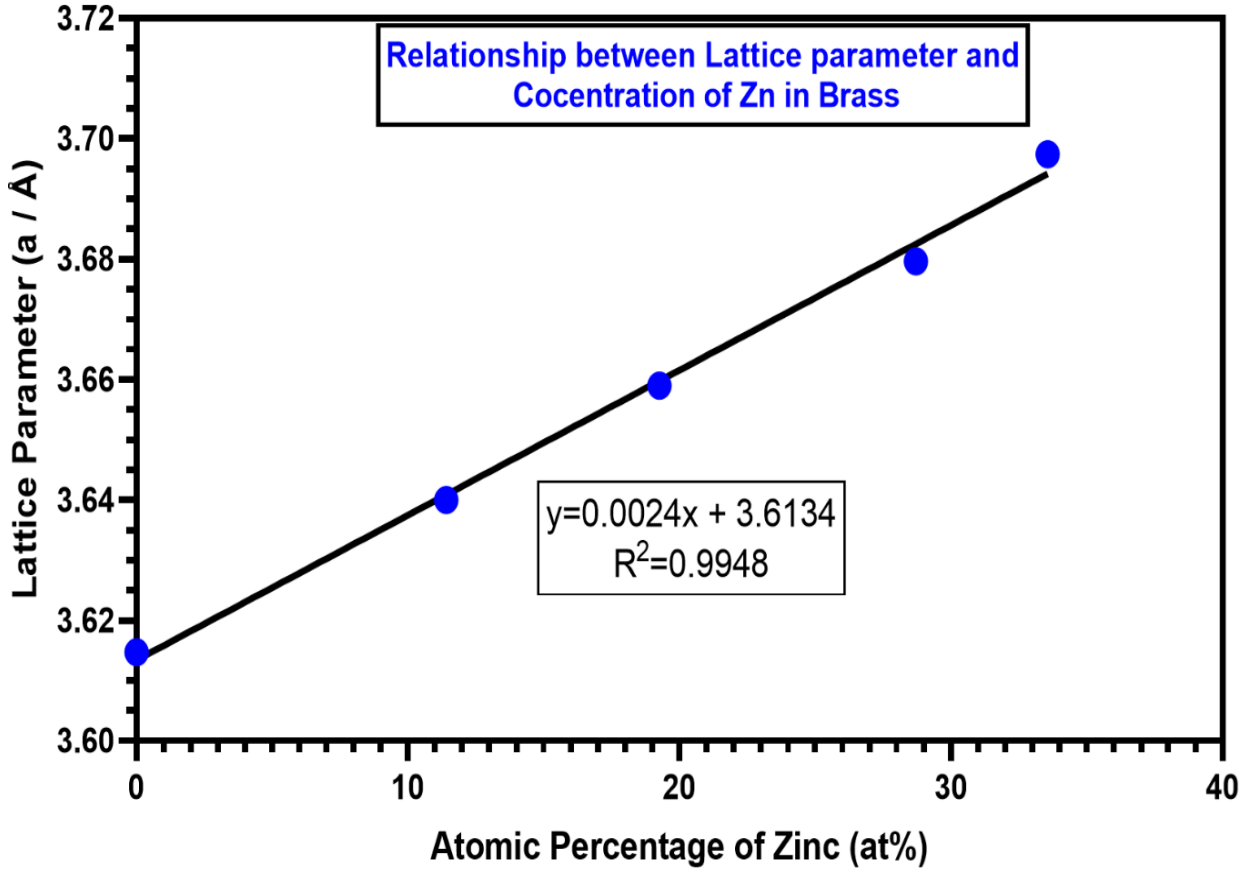

Figure 3.6. Relationship between lattice parameters and concentration of Zn in Cu-Zn alloy.

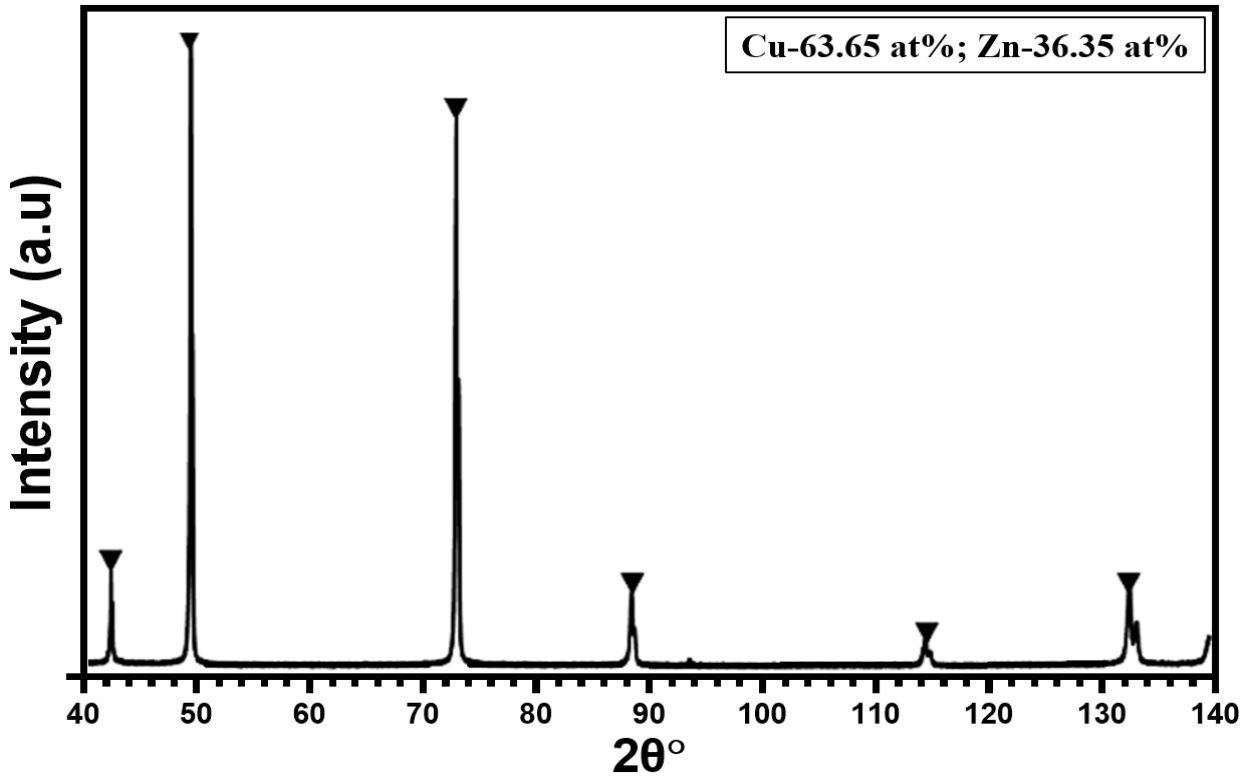

Figure 3.7. XRD scan of the brass sample of 63.65 at% Cu and 36.35 at% Zn.

Table 1. Calculation of brass composition from k-series counts of the standard and alloy sample.

Standard/Specimen Spectra	K-series Net (counts)		Initial Brass/Standard specimen ratio		Normalised Brass/Standard specimen ratio		Relative %error	
Element	Copper (Cu)	Zinc (Zn)	Copper (Cu)	Zinc (Zn)	Copper (Cu)	Zinc (Zn)	Copper (Cu)	Zinc (Zn)
Pure Cu (std) Mean/average Count Value	138761	--	61.69	--	62.88	--	-0.19	--
Pure Zn (std) Mean/average Count Value	--	112718	--	36.42	--	37.12	--	0.12
Brass Specimen Mean/average Count Value	85608	41053	--	--	--	--	0.06	0.14

The nominal true composition and measured (after normalization) values were used to calculate the error, which is shown as -0.19% for Cu and +0.12% for Zn. Table 1 shows quantitative analysis of the chemical composition of brass sample calculated from the counts of pure standard and alloy. Employing XRD as a chemical analysis tool is based on the idea of change in lattice parameters due the difference in atomic radii of the alloying elements[5]. In this regard, formation of a new solid solutions is a common occurrence in binary alloys composed of two elements of almost similar atomic size, valence, and crystal structure. At any composition, these elements can mix in a random manner to form a homogeneous alloy. Practically, atoms in the new solution are different in atomic size that leads to alteration of the crystal lattice, and hence alter the direction of the diffracted x-rays beam in diffractogram. By taking total derivative of Bragg's law the relationship between the changes in angular position (Δθ) of diffracted beam and change in lattice parameter (a_0) can be established.

$$\frac{\Delta d}{d} = \frac{\Delta a_0}{a_0} = -cot\theta\Delta\theta \qquad \textit{Equation (2)}$$

This relationship (Equation (2)) can be applied to determine the lattice constant and can be used to estimate the composition of binary alloy. In a random substitutional solid solution, the chemical composition of the binary alloy is expected to lie between the lattice constants of the pure elements. If dependence of lattice parameter is linear with fraction of substitutional atoms in a binary alloy system obeys Vegard's law [6] and is expressed as follows in Equation (3),

$$a_{AB} = X_A a_A + (1 - X_A) a_B \qquad \textit{Equation (3)}$$

Where X_A and X_B are the atomic fraction of atoms A and B, while a_A and a_B are the lattice parameters of pure elements and a_{AB} is lattice parameter of the alloy. Once the locations of the peaks were found the indexed peaks can then be used to determine the lattice parameters of each peak using Braggs Law. However, in some cases binary solutions don't follow linearity of Vegard's law and Equation (2) is applied. When considering Equation (2)Equation (1) it indicates improved experimental precision with higher angles, therefore we have to assign higher-weightage to these higher-angle peaks when determining the lattice constant. To achieve this, we "reduce the data" by establishing a correlation between the calculated lattice constants and a function that predicts the expected precision. In a comprehensive error analysis conducted by Nelson and Riley [7], they established the relationship.

$$\frac{\Delta a}{a} = K\left(\frac{cos\theta^2}{sin\theta} + \frac{cos\theta^2}{\theta}\right) \qquad \textit{Equation (4)}$$

This co-relation accurately predicts the precision of a given measurement. In this research work, we utilized the indexed peaks and calculated preliminary lattice parameter for each peak. To determine the lattice constant, we plot the calculated lattice parameter (a) values against the Nelson-Riley function as shown in **Error! Reference source not f ound.**. By constructing a linear regression analysis, we can determine the y-intercept, which corresponds to the point where the Nelson-Riley function, and consequently, the fractional change in lattice parameter (Δa/a), approaches zero. Based on this analysis lattice parameter for sample under observation found to be 3.69 Å. The relationship between the concentration of Zn in brass and Lattice parameter is shown in **Error! Reference source not found.**. Brass alloy of v arying Zn concentration was made from 99.99 at% Cu and Zn casted and homogenized at 650 °C for finding lattice parameters. Lattice parameters of annealed brass alloy reported by Rao and Anantharaman (1963) in their interesting work done on Cu-solid solution. From this relationship in **Error! Reference source not found.** and using the lattice p arameter obtained through N-R function composition of unknown brass alloy sample in this work was found to be 34.65756 at%. Concentration of Zn found through this method is 6.33 at% lower than the nominal composition. However, while using EDS for chemical analysis of same brass alloy Zn concentration was found to be 37.12 at% as opposed to 34.66 at% Zn while using XRD as chemical analysis tool. This discrepancy in results is because XRD is good in determining crystal structure of materials but is not a reliable tool for chemical analysis of the materials.

3.3. Structural analysis

XRD scan for the sample obtained analyzed for the structural analysis of the brass alloy sample (**Error! R eference source not found.**). The obtained spectrum exhibited α-phase with FCC crystal structure. However, from the analysis of the XRD scan no traces of β-phase found as opposed to the black spots in SEM images (
Figure ***3.1***). The reason of no detection of the β-phase may be its lower quantity (<5%) as XRD is less-sensitive to presence

of minor phases[8]. Here it can be argued that the plastic deformation and necking of the brass fractured sample observed in SEM analysis of the broken sample is due to the FCC crystal structure. As FCC lattice structure has more slip planes in its slip system than other cubic lattice structures.

4. Conclusions

A materials characterization study was conducted on two brass samples of unknown composition from same piece of alloy, one of which underwent fracture. Study focused on imaging through SEM analysis, elemental composition via EDX, and crystal arrangement by XRD. Techniques employed to identify failure mechanism and deformation sample experienced. Key conclusions drawn from study:

- SEM fractographs and grain analysis revealed a ductile cup-and-cone fracture structure in the brass sample.
- The specimen's composition is consistent with its nominal composition of 63.65 at% Cu and 36.35 at% Zn.
- The sample's crystal structure was confirmed as FCC, which aligns with its observed ductility and plastic deformation prior to fracture.
- Evidence of annealing twinning in the SEM analysis confirms that the material underwent an annealing process, indicative of its processing history.
- The FCC structure and the annealing process both contributed to the material's increased ductility, as shown by the sample's ductile fracture morphology.
- The composition determined through EDS aligns well with the Cu-Zn phase diagram, and assumptions from XRD lattice parameters provided an approximate composition, though the EDS results were considered more reliable for determining the chemical composition.

References

[1] A. Kolagar, N. Tabrizi, M. Cheraghzadeh, M. Shahriari. (2017). Failure analysis of gas turbine first stage blade made of nickel-based superalloy. Case studies in engineering failure analysis. 8: 61-68.

[2] H. Bayrakceken. (2006). Failure analysis of an automobile differential pinion shaft. Engineering Failure Analysis. 13(8): 1422-1428.

[3] K.R. Kaufmann. (2021). Accelerating Material Discovery and Analysis Using Machine Learning. University of California, San Diego: pp.

[4] M. Fernandes, J.M. Corchado, G. Marreiros. (2022). Machine learning techniques applied to mechanical fault diagnosis and fault prognosis in the context of real industrial manufacturing use-cases: a systematic literature review. Applied Intelligence. 52(12): 14246-14280.

[5] S.-b. Zhou, C.-y. Hu, F. Hu, L. Cheng, O. Isayev, S. Yershov, H.-j. Xiang, K.-m. Wu. (2022). Insight into the impact of microstructure on crack initiation/propagation behavior in carbide-free bainitic steel during tensile deformation. Materials Science and Engineering: A. 846: 143175.

[6] S.P. Raut, L.P. Raut. (2014). A review of various techniques used for shaft failure analysis. International Journal of Engineering Research and General Science. 2(2): 2091-2730.

[7] F.C. Campbell. (2008). Elements of metallurgy and engineering alloys. ASM international: pp.

[8] X.X. Wu, Y.L. Gong, S.Y. Ren, J.M. Tao, Y. Long, L.P. Cheng, X.K. Zhu In *Effect of annealing on mechanical properties of copper alloys deformed at cryogenic temperature*, Materials Science Forum, 2013; Trans Tech Publ: 2013; pp 363-370.

[9] N. Pugacheva, A. Pankratov, N.Y. Frolova, I. Kotlyarov. (2006). Structural and phase transformations in α+ β brasses. Russian Metallurgy (Metally). 2006: 239-248.

[10] C.P. Sharma. (2003). Engineering materials: properties and applications of metals and alloys. PHI Learning Pvt. Ltd.: pp.

[11] I. Volokitina, A. Naizabekov. (2020). CuZn36 brass microstructure and mechanical properties evolution at equal channel angular pressing. J. Chem. Technol. Metall. 55(3).

[12] G.A. Pantazopoulos. (2019). A short review on fracture mechanisms of mechanical components operated under industrial process conditions: Fractographic analysis and selected prevention strategies. Metals. 9(2): 148.

[13] D.E. Newbury, N.W. Ritchie. (2015). Performing elemental microanalysis with high accuracy and high precision by scanning electron microscopy/silicon drift detector energy-dispersive X-ray spectrometry (SEM/SDD-EDS). Journal of materials science. 50: 493-518.

[14] J.B. Nelson, D. Riley. (1945). An experimental investigation of extrapolation methods in the derivation of accurate unit-cell dimensions of crystals. Proceedings of the Physical Society. 57(3): 160.